

Bouncing of a dispersive pulse on an accelerating soliton and stepwise frequency conversion in optical fibers

A.V. Gorbach and D.V. Skryabin

Centre for Photonics and Photonic Materials, Department of Physics, University of Bath, Bath
BA2 7AY, UK

d.v.skryabin@bath.ac.uk

Abstract: We demonstrate that a short pulse with spectrum in the range of normal group velocity dispersion can experience periodic reflections on a refractive index maximum created by a co-propagating with it soliton, providing the latter is continuously decelerated by the intrapulse Raman scattering. After each reflection the intensity profile and phase of the pulse are almost perfectly reconstructed, while its frequency is stepwise converted. This phenomenon has direct analogy with the effect of 'quantum bouncing' known for cold atoms.

© 2007 Optical Society of America

OCIS codes: (060.5530) Pulse propagation and solitons; (190.5650) Raman effect

References and links

1. G. P. Agrawal, *Nonlinear Fiber Optics* (Academic Press, 2001), 3rd ed.
2. A. Gorbach and D.V. Skryabin, "Light trapping in gravity-like potentials and expansion of supercontinuum spectra in photonic crystal fibers," *Nature-Photonics* **1** (2007); DOI: 10.1038/nphoton.2007.202; <http://xxx.lanl.gov/abs/0706.1187>.
3. A. Gorbach and D.V. Skryabin, "Theory of radiation trapping by the accelerating solitons in optical fibers," *Phys. Rev. A* (to be published); <http://xxx.lanl.gov/abs/0707.1598>.
4. P. Beaud, W. Hodel, B. Zysset, and H.P. Weber, "Ultrashort pulse-propagation, pulse breakup, and fundamental soliton formation in a single-mode optical fiber," *IEEE J. Quantum Electron.* **23**, 1938–1946 (1987).
5. N. Nishizawa and T. Goto, "Experimental analysis of ultrashort pulse propagation in optical fibers around zero-dispersion region using cross-correlation frequency resolved optical gating," *Opt. Express* **8**, 328–334 (2001).
6. A.V. Gorbach, D.V. Skryabin, J.M. Stone, and J.C. Knight, "Four-wave mixing of solitons with radiation and quasi-nondispersive wave packets at the short-wavelength edge of a supercontinuum," *Opt. Express* **14**, 9854–9863 (2006).
7. J. Gea-Banacloche, "A quantum bouncing ball," *Am. J. Phys.* **67**, 776 (1999).
8. C. V. Saba, P. A. Barton, M. G. Boshier, I. G. Hughes, P. Rosenbusch, B. E. Sauer, and E. A. Hinds, "Reconstruction of a cold atom cloud by magnetic focusing," *Phys. Rev. Lett.* **82**, 468–471 (1999).
9. K. Bongs, S. Burger, G. Birkl, K. Sengstock, W. Ertmer, K. Rzazewski, A. Sanpera, and M. Lewenstein, "Coherent evolution of bouncing Bose-Einstein condensates," *Phys. Rev. Lett.* **83**, 3577–3580 (1999).
10. K.J. Blow, N.J. Doran, and D. Wood, "Suppression of the soliton self-frequency shift by bandwidth-limited amplification," *J. Opt. Soc. Am B* **5**, 1301–1304 (1988).
11. L. Gagnon and P.A. Belanger, "Soliton self-frequency shift versus Galilean-like symmetry," *Opt. Lett.* **15**, 466–468 (1990).
12. I. S. Averbukh and N. F. Perelman, "Dynamics of wave-packets from highly excited atomic and molecular-states," *Usp. Fiz. Nauk* **161**, 41–81 (1991).
13. D. V. Skryabin and A. V. Yulin, "Theory of generation of new frequencies by mixing of solitons and dispersive waves in optical fibers," *Phys. Rev. E* **72**, 016619 (2005).

Solitons in optical fibers experience intrapulse Raman scattering, resulting in the continuous frequency shift towards larger wavelengths as they propagate along the fiber [1]. Under

conditions of anomalous group velocity dispersion (GVD) the group velocity decreases with wavelength. Hence the Raman shifted solitons slow down with constant acceleration. The solitons, via nonlinear part of polarization, locally increase the refractive index. Also, the negative acceleration of the Raman solitons in fibers implies presence of an additional effective linear increase of the refractive index between the soliton front and trailing edges [2, 3]. So that the overall refractive index acquires a minimum at the trailing edge, see Fig. 1, and hence pulses with spectrum belonging to the normal GVD range can be attracted towards and trapped in this minimum [2, 3]. The above linear potential is analogous in its nature to the inertial forces present in accelerating frames of reference and well known in classical mechanics.

Recently we have analyzed linear and nonlinear modes of the radiation trapped in the refractive index minimum on the trailing edge of the Raman solitons [2, 3]. The trapped radiation slows down together with the soliton. However, for normal GVD, the smaller group velocities correspond to the shorter wavelengths. Therefore, the trapped radiation is continuously blue shifting, while the soliton is red shifting. This explains blue shift of the short-wavelength of the supercontinua observed in photonic crystal fibers [2, 3, 6]. Blue shift of the pulses in the normal GVD range correlated with the red shifting solitons has been experimentally observed in [4, 5] well before the corresponding theory revealing underlying physical principles has been developed.

It is known from quantum mechanics that the mode expansion is not always the best approach to understand dynamics of wavepackets inside potentials. One of the examples of such a problem is a 'quantum bouncer' [7]. It is a situation, when a localized and shifted far from the potential minimum, i.e. highly multimode, quasi-classical wavepacket rolls down a linear potential towards and gets reflected from a potential barrier and, after some time, reconstructs itself in the original location. One of the famous realizations of a quantum bouncer so far has been an atomic cloud subject to the field of gravity bouncing on an atom mirror [8, 9]. In this work we predict and study an all optical analog of the quantum bouncer, when a multimode wavepacket bounces on the accelerating soliton. An important feature of this process is that each reflection from the soliton is accompanied by the stepwise (not continuous) frequency transformation of the wavepacket.

We consider an optical fiber which is pumped by two pulses with frequencies across the zero GVD point. The scaled electric field is assumed in the form $\mathcal{E} = E e^{ik_0 z - i\omega_0 t} + c.c.$, where ω_0 is the zero GVD frequency, k_0 is the corresponding wavenumber and $E = A_1 \exp[ik_1 z - i\delta_1 t] + A_2 \exp[ik_2 z - i\delta_2 t]$. Here $A_{1,2}$ are the slowly varying amplitudes of the two pulses, $\delta_{1,2}$ are their frequency detunings from ω_0 and $k_{1,2} = k(\delta_{1,2})$ are the corresponding wavenumbers determined via the fiber dispersion. We also assume that $\delta_{1,2}$ are selected in such a way that $k'_1 = k'_2$ ($k' = \partial_\delta k$) and therefore the initial group velocities of the two pulses are equal. In photonic crystal fibers such group velocity matching is possible across the wide bandwidth [6]. Normalized equations for $A_{1,2}$ are

$$i\partial_z A_{1,2} + d_{1,2} \partial_x^2 A_{1,2} = - [|A_{1,2}|^2 + 2|A_{2,1}|^2] A_{1,2} + T A_{1,2} \partial_x [|A_1|^2 + |A_2|^2], \quad (1)$$

where $x = (t - zk'_1) / \sqrt{|k''_1|}$, t is the dimensionless time in the reference frame moving with the light group velocity at ω_0 and measured in the units of the input pulse duration $\tau \sim 200 fs$, z is the distance along the fiber measured in the units of any convenient characteristic length l , $T = |k''_1|^{-1/2} \int_0^\infty t R(t) dt$ is the Raman parameter and $R(t)$ is the Raman response function for silica [1], $d_1 = 1/2$ (anomalous GVD) and $d_2 = -|k''_2| / |2k''_1| < 0$ (normal GVD). The fact that GVDs of both components are assumed to be frequency independent is not critical for the effects described below. Choosing $l = 50 cm$ and the fiber nonlinear parameter $\gamma = 0.1/W/m$, which is typical for small core PCFs [6], imply that the unit value of $|A_{1,2}|^2$ corresponds to $1/\gamma/l = 20W$ in physical units.

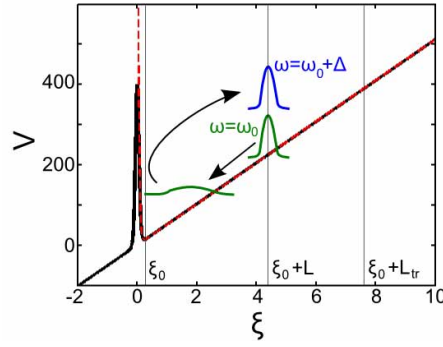


Fig. 1. Solid (dashed) line corresponds to the soliton induced refractive index change (effective potential $V(V_b)$) in the accelerating frame of reference: $q = 100$, $d_2 = -1/2$. Initial localized pulse is detuned by L from the minimum at ξ_0 . After reflection from the soliton, the pulse is reconstructed at the initial position, but its frequency is shifted by Δ . L_{tr} is the time delay such, that the linear potential equals the soliton peak.

Assuming $A_2 \equiv 0$, one can show that Eq. (1) has an approximate solution in the form of the NLS soliton moving with the constant acceleration g [1, 10, 11]:

$$A_1^{(s)} = \psi_0(\xi) \exp \left[i \frac{\xi g z}{2d_1} - i \frac{g^2 z^3}{12d_1} + i q z \right], \quad (2)$$

$$\psi_0 = \sqrt{2q} \operatorname{sech}(\sqrt{q/d_1} \xi), \quad \xi = x - \frac{g z^2}{2}, \quad g = \frac{32Tq^2}{15}. \quad (3)$$

Here $q > 0$ is the soliton parameter. As it has been demonstrated, e.g., in [11], the NLS-type equation for ψ_0 resulting from the above substitution acquires a potential term varying linearly in ξ . It is important to realize that the substitution similar to Eq. (2) can be applied not only to the soliton, but in general for a linear or nonlinear Schrödinger equation with any sign in front of the dispersion term.

Let us first consider the case of a weak amplitude A_2 component added to the soliton. Then Eqs. (1) can be linearized for A_2 , and the soliton enters this equation as an external potential moving with acceleration. It is convenient to transform into the accelerating frame of reference, where the soliton is stationary [2, 3]:

$$A_2 = \phi(z, \xi) \exp \left[i \frac{\xi g z}{2d_2} - i \frac{g^2 z^3}{12d_2} \right]. \quad (4)$$

Eqs. (2,3) and (4) explicitly express the fact that the continuous deceleration of the pulses ($g > 0$) is accompanied by the red frequency shift in the case of anomalous GVD ($d_1 > 0$) and by the blue shift if GVD is normal ($d_2 < 0$).

The resulting equation for ϕ is

$$i \partial_z \phi - |d_2| \partial_\xi^2 \phi + V(\xi) \phi = 0, \quad (5)$$

where potential $V(\xi)$ consists of the localized soliton part and of the linear potential induced by the acceleration:

$$V(\xi) = 2\psi_0^2 - T \partial_\xi \psi_0^2 + \frac{g\xi}{2|d_2|}. \quad (6)$$

The superposition of the exponentially decaying soliton tail and of the linear potential induced by the acceleration creates a local minimum of V on the trailing tail of the soliton, see Fig. 1.

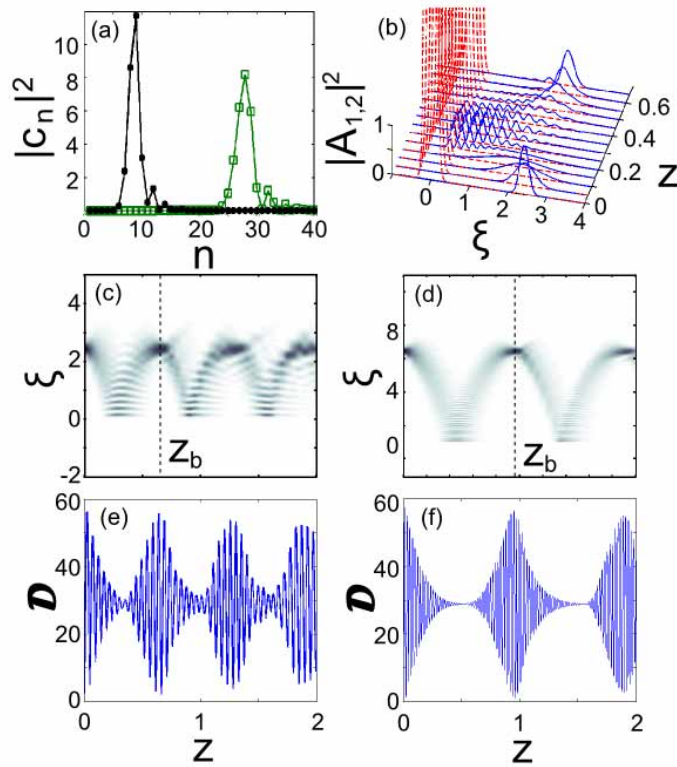


Fig. 2. Numerical propagation of the gaussian pulse (8) with $a = 1$ and different displacements: $L = 2$ and $L = 5$. Model parameters are the same as in Fig. 1. (a) Expansion coefficients c_n of the gaussian. Filled circles correspond to $L = 2$, open squares to $L = 5$. (b) time-domain evolution within Eqs. (1) for $L = 2$. A_1 (dashed red lines) is initialized with the soliton (3), $q = 100$. Full blue lines show A_2 . (c), (d) time-domain evolution of $|A_2|^2$ along the fiber calculated using linearized Eq. (5) for $L = 2$ and $L = 5$, respectively. ; (e), (f) deviation from the initial pulse $\mathcal{D}(z)$, calculated using the expansion in Eq. (7).

There exist a set of quasi-bound modes of V localized around the minimum ξ_0 and having oscillating tails which decay slowly at $\xi \rightarrow -\infty$ [3]. The latter is the direct consequence of the fact that the soliton created potential wall is not infinite and light can tunnel through it. For parameters typical for femtosecond solitons the rate of tunneling is small and the number of quasi-bound modes of V can be as high as several dozens [2]. Under these conditions the potential V can be well approximated by $V_b(\xi) = 16q \exp(-2\sqrt{q/d_1}\xi) + g\xi/(2|d_2|)$, where the soliton part has been replaced by its exponential asymptotic. Then the amplitude ϕ can be approximated with

$$\phi(z, \xi) \approx \sum_n c_n y_n(\xi) \exp(i\lambda_n z). \quad (7)$$

where $y_n(\xi)$ are the eigenmodes of V_b , λ_n are the corresponding eigenvalues, $-|d_2|\partial_\xi^2 y_n + V_b y_n = \lambda_n y_n$, and the summation is truncated when n reaches the number of the last quasi-bound state of V .

Let us now consider the gaussian pulse localized on the same scale as y_0 and shifted by the

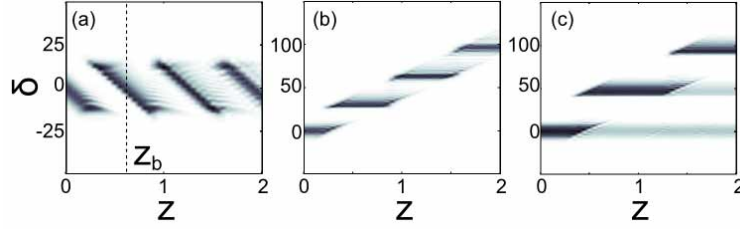


Fig. 3. Spectral evolution within the linearized Eq. (5), (a), and coupled Eqs. (1), (b) and (c). Initial delay of the gaussian pulse is $L = 2$ for (a) and (b) and $L = 5$ for (c). Initial amplitude is $a = 1$.

distance L from the minimum of the potential:

$$\phi(\xi, z = 0) = a \exp \left[-\frac{(\xi - \xi_0 - L)^2}{w^2} \right]. \quad (8)$$

For sufficiently large initial displacements $L \gg w$, but $L < L_{tr}$ (see Fig. 1), the expansion of the gaussian into y_n requires taking into account large values of n , see Fig. 2(a). Then, the expected evolution of the wavepacket should be close to the evolution of a classical particle (correspondence principle). Namely, the pulse initially should roll down the linear potential, reflect from the soliton created potential wall, move upwards, fall down again and so on. This bouncing dynamics has been found in the direct numerical integration of the coupled Eqs. (1), see Fig. 2(b). The same bouncing is more clearly seen in the integration of the linearized Eq. (5), see Figs. 2(c), (d). A notable feature of the bouncing effect is almost perfect reconstruction of the initial pulse after the bouncing period $Z_b \sim 2\sqrt{2L/g}$. The latter estimate for the period is readily derived using analogy with the Newtonian particle which travels the distance L with acceleration g and zero initial velocity and then bounces back returning into its initial position. For the two cases of different initial deviations L shown in Fig. 2 it gives $Z_b \approx 0.56$ and $Z_b \approx 0.89$, respectively.

To quantify the effect of the wavepacket reconstruction we introduce the function $\mathcal{D}(z) \equiv \int d\xi |\phi(\xi, z) - \phi(\xi, 0)|^2$, which measures the deviation of the pulse from its initial profile with propagation distance. Using (7) we derive a rather simple expression for $\mathcal{D}(z)$ [12]: $\mathcal{D}(z) \approx 2 \sum_n |c_n|^2 [1 - \cos(\lambda_n z)]$. One can see, Fig. 2(e) and (f), that $\mathcal{D}(z)$ evolves almost periodically and comes fairly close to zero after each bouncing period Z_b . This indicates that not only the intensity profile is restored (as seen in Figs. 2(a)-(c)), but also is the phase.

If we assume the quantum mechanical context for Eq. (5), then the pulse frequency δ plays the role of the particle momentum. Thus, the frequency of ϕ evolves in two sequentially repeated stages: linear decrease (particle rolls down the potential) and stepwise jump (elastic reflection from the soliton induced barrier), see Fig. 3(a). The linear change of frequency seen in Fig. 3(a) between the jumps is the result of transformation (4), while the jumps are intrinsic. In an inertial frame of reference the frequency of the bouncing pulse remains fixed between the jumps, see Fig. 3(b), (c). The straightforward estimate for frequency change during the jump is $\Delta = gZ_b/|d_2|$. One jump in Figs. 3(b,c) corresponds to the frequency change order of 0.1 THz in physical units. Thus, after each period Z_b , the pulse is almost completely restored in time domain, but its frequency is discretely shifted by Δ . The overall process is schematically shown in Fig. 1. Note, that the reflections of the radiation from the soliton are not perfect, so that a portion of radiation escapes after each collision. Naturally, this becomes more pronounced for larger values of L , see Fig. 3(c).

Increasing the intensity of the dispersive pulse, one can see that the interaction between the

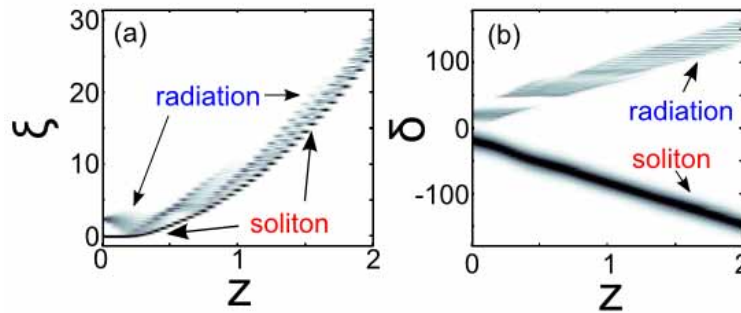


Fig. 4. Temporal (a) and spectral (b) evolution of the radiation bouncing on the soliton calculated using Eqs. (1) and transformed into the ξ coordinate system. The plots show (a) the intensity of the total field $A_1 \exp[ik_1 z - i\delta_1 t] + A_2 \exp[ik_2 z - i\delta_2 t]$ and (b) its spectrum with $\delta_2 = -\delta_1 = 20$. Initial pulse amplitude $a = 5$ is larger than in the previous cases in Figs. 2,3. Other parameters are the same as in Fig. 2(b).

pulse and the soliton starts to influence dynamics of both components (Fig. 4). The soliton frequency changes slightly (Fig. 4(b)) after each interaction, which leads to the corresponding velocity shifts with the net effect being the soliton drifting towards the pulse in the frame of reference moving with the acceleration g , see Fig. 4(a). As a result, the amplitude of the pulse oscillations becomes smaller, and eventually the pulse gets trapped, forming a bound state with the soliton [2, 3]. Analysis of numerical data suggests that this happens not due to tunneling related losses of the energy and momentum, but due to nonlinear, in the pulse amplitude, corrections to the acceleration parameter g , which have been disregarded in the above consideration.

The above results do not depend on the sign of the detuning between the radiation and soliton. The radiation frequency universally becomes bluer and the soliton frequency universally gets redder. So that the relative detuning between them can either decrease or increase with propagation depending on how the GVD sign changes with frequency (from normal to anomalous, or vice versa).

The frequency conversion resulting from the dispersive wave scattering on a soliton has been previously considered in [13]. Ref. [13] is focused, however, on the situation when the group velocities of the incident and scattered waves are very different from the soliton velocity. Under these conditions the GVD terms in the radiation equations and the adiabatic change of the soliton velocity due to Raman effect can be neglected relative to the group velocity mismatch. In the present case, however, the group velocities of the radiation and soliton are close. Then the soliton acceleration and GVD can not be neglected, and the complex dynamics described above is revealed. This case has been outlined as a special one in the Appendix B of [13] (cf. Eq. (B5) in [13] and Eqs. (5,6) above).

In summary, we have demonstrated and explained the effect of a dispersive pulse bouncing and periodically reconstructing its shape on the trailing tail of a Raman soliton propagating in an optical fiber with zero GVD wavelength. The bouncing takes place in time domain and is accompanied by the stepwise conversion of the pulse frequency. Our results complement in a non-trivial way our previous theory [2, 3] of the continuous (as opposite to the stepwise) blue shift of the radiation trapped by the red shifting Raman solitons.